Int. J. Electrochem. Sci., 15 **(2020)** 2685 – 2699, doi: 10.20964/2020.03.34

International Journal of
ELECTROCHEMICAL
SCIENCE
www.electrochemsci.org

Investigation of Adsorption and Inhibitive Effect of Expired Helicure Drug on Mild Steel Corrosion in Hydrochloric Acid Solution

Samar .Y. Al-Nami

Chemistry Department, Science College for Girls, King Khalid University, Abha, KSA
E-mail: salnamee@kku.edu.sa

Received: 7 November 2019 / *Accepted:* 22 December 2019 / *Published:* 10 February 2020

The inhibiting impact of expired Helicure drug (EHD) on the dissolution of mild steel (MS) in 1 M HCl was evaluated using weight loss (WL) and electrochemical methods. The outcome data displayed that this drug was adsorbed physically on MS surface following Langmuir isotherm. Some thermodynamic factors computed and discussed. The obtained data designated that the protection efficiency (PE) improved by raising the concentrations of the drug and lowered by raising the temperature of the medium. The maximum protection efficiency 85.8% was detected in the existence of 300 ppm EHD (in case of polarization). The analysis of MS surface are performed by utilizing scanning electron microscope (SEM), Fourier transform Infrared spectroscopy (FTIR) and atomic force microscopy (AFM) tests. All obtained results from different techniques are almost similar.

Keywords: Acid corrosion, Mild steel, Expired Helicure drug, SEM, AFM, FTIR

1. INTRODUCTION

The ecological importance of corrosion is huge and its protection had intensely examined. Hydrochloric acid is commonly utilized in various scientific procedures in industry, e.g., in bath pickling, proceeding of oil and in other chemical and petrochemical productions. Corrosion in MS is significant and costly problem in the manufacturing and it signifies an important portion of loss as a result of missing production. Several acids solutions (HCl, H_2SO_4, Sulfamic, and H_3PO_4) had utilized for deletion of unwanted scale and rust in many manufacturing procedures. Inhibitors has commonly utilized in these procedures to control Fe and Fe alloys dissolution as well as the consumption of acid [1, 2]. Numerous inhibitors utilized are either created from low-cost material or selected from composites having hetero atoms in their long-chain carbon or aromatic system [3]. Most of organic inhibitors are costly, toxic and have negative effect on the dissolution of metal. Thus it is significant and

essential to develop environmentally safe and low cost corrosion protection [4]. Organic heterocyclic compounds had utilized for the prevention of C-steel corrosion [5-10], Cu [11], Al [12-14], and other metals [15] in different aqueous media. The drug adsorption facilitated to protect the surface of metal [16]. In recent years the drugs were used as corrosion prevention for various metals result to their nontoxic nature [17-19]. Adsorption of the drug molecules on the surface of metal facilitates its protection [20]. Recently, numerous research have been performed on the protection of metals corrosion by drugs compounds [21-29].

The target of this paper is to test the protective performance of expired Helicure drug towards the dissolution of MS in 1M HCl utilizing chemical, electrochemical studies and surface morphologies.

2. MATERIALS AND METHODS

2.1. Metal sample

MS is composed from the following: 0.15% C, 0.003% Si, 0.024% P, and 0.350% Mn, the rest Fe.

2.2. Chemicals

Inhibitor –Helicure drug which was purchased from AMRIYA PHARM Company, Alex, Egypt and used as received without any treatment

Helicure two compound (Omeprazole/ Tinidazole)	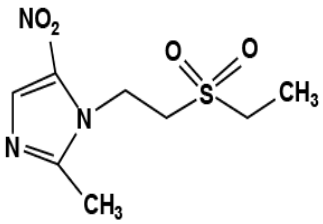 $C_8H_{13}N_3O_4S$ **247.273 g/mol**	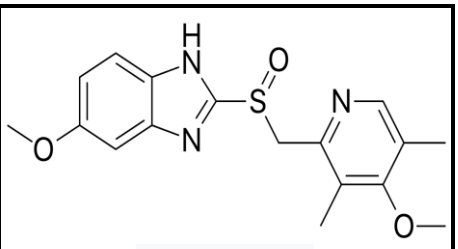 **$C_{17}H_{19}N_3O_3S$** **345.42 g/mol**

2.3. Solutions

The aggressive solution is 1M HCl (37% BDH grade)

2.4. Weight loss (WL) technique

The utilized samples in WL were with magnitude of (20 mm x 20 mm x 0.2 cm). The samples were scraped one after another with various succession of emery sheets of dissimilar grades starting from the 320 to 1200 grade, dry-cleaned with acetone as well as air-dried. The mass reduction experiments

was completed in a 100 ml 1 M HCl mixtures with and without various concentrations of the detected extract. The (% PE) and the surface coverage (θ) of Helicure drug for the MS corrosion were measured as below [30]:

$$\% PE = [1- (W/ W^0)] \times 100 = \theta \text{ x } 100 \quad (1)$$

Where, W^0 and W are the dissolution ratios of MS with and without Helicure drug, correspondingly

2.5. Potentiodynamic polarization (PP) method

PP tests were achieved in a classic three-electrode cell utilizing the counter electrode, the reference electrode and working electrode. The working electrode was made from the same used MS sheet in chemical method, the area of exposed surface was 1 cm^2, and the electrode surface was treated in the same procedure as in the weight loss method. Then, the electrode was dipped in tested solution at the open-circuit potential (OCP) for 1/2 hr till a steady state was obtained. Computations taken as a function of current densities, the %IE for each dose of the *EHD* was estimated using the next equation [31]:

$$PE \% = \theta \text{ x } 100 = [1- (i_{corr(inh)} / i_{corr(free)})] \times 100 \quad (2)$$

Where, $i_{corr(free)}$ and $i_{corr(inh)}$ are the dissolution current densities estimated from the Tafel slopes without and with *EHD*, correspondingly .

2.6. Electrochemical impedance spectroscopy (EIS) method

Impedance (EIS) was processed utilizing the same cell ordered as mentioned before in PP. EIS estimations were proved utilizing AC signals with an amplitude of 5 mV peaks at the open circuit potential (OCP) in the frequency range of 100 kHz to 0.1 Hz. All impedance results were agreed to the convenient equivalent circuit utilizing the software of Gamry Echem Analyst, the double layer capacitance (C_{dl}) and PE and the θ were measured as a function of the estimated R_{ct} as:

$$C_{dl} = 1/ (2 \pi f_{max} R_{ct}) \quad (3)$$

Where, f_{max} is the maximum frequency.

$$PE \% = \theta \text{ x } 100 = [1- (R^{\circ}_{ct}/R_{ct})] \times 100 \quad (4)$$

Where, R^{o}_{ct} and R_{ct} are the charge transfer resistances without and with various concentrations of EHD, correspondingly

2.7. Electrochemical frequency modulation (EFM) technique

EFM tests were attained with applying potential with two sine waves of 2 and 5 Hz [32]. The larger bands were utilized to measure the (i_{corr}), (β_c and β_a) and the causality factors CF2 and CF3 [33]. The % PE_{EFM} and θ were calculated from Eq.(2).

All electrochemical trials were performed expending Gamry instrument PCI300/4 Potentiostat/Galvanostat/Zra analyzer, DC105, EIS300 and EFM140 software were utilized for PP, EIS and EFM techniques, respectively

2.8. Surface analysis

The MS coins used for examination of the surface were dipped in acid (blank) and with 300 ppm of Helicure drug for 24 hours. Then, after this dipping time, the coins had cleaned gently with bi-distilled water, dried and attached into the desiccators until use in examining by utilizing (SEM) and (AFM).

3. RESULTS AND DISCUSSION

3.1. WL measurements

WL of MS in mg cm^{-2}, was measured at different time periods with and without different concentrations (50-300 ppm) of the drug. The curves obtained with various concentration of EHD fall below that of free acid as shown in Figure 1. The % PE's are verified in Table 1. The %PE of the EHD improved with raising the concentrations of the drug and the rate of dissolution was lowered. These obtained data indicate that, EHD is best effective inhibitor for MS. When the temperature rises desorption of EHD from the MS surface may occur, leaving the surface to corrode and hence, %PE decreased.

Table 1. (% PE) and (Ɵ) at various concentrations of EHD for the dissolution of MS after 120 min at 25ºC

Conc, ppm	θ	% PE
Blank	----	----
50	0.637	63.7
100	0.674	67.4
150	0.706	70.6
200	0.749	74.9
250	0.792	79.2
300	0.832	83.2

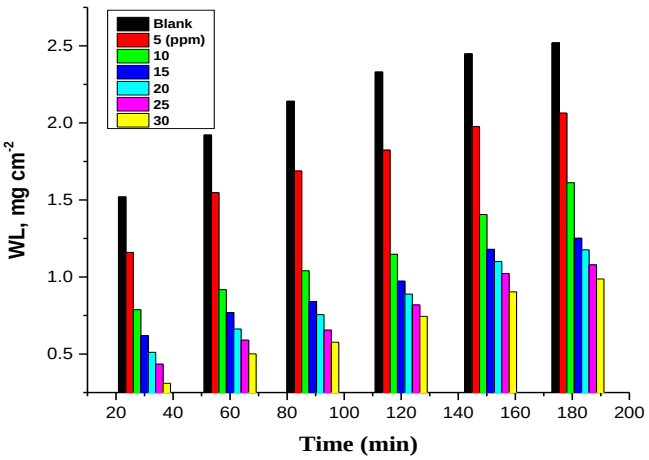

Figure 1. Time-WL plots for the dissolution of MS with and without various EHD concentrations at 25ºC

3.2. Temperature Impact

The influence of temperature on the MS dissolution in 1 M HCl without and with different concentrations of EHD was tested in the range of temperature 25–45ºC utilizing WL tests. As the temperature rises, the dissolution rate of MS decreases. Table 2 illustrates that the % PE is decreased by raising the temperature. This demonstrates that the EHD adsorption on MS surface is weaken by raising the temperature and designates that the molecules of drug are adsorbed physically on MS surface [34].

Table 2 Dissimilarity of (%IE) and (θ) for different concentrations of the EHD at different temperatures.

Temp. ºC	(30ºC)		(35ºC)		(40ºC)		(45ºC)	
Conc, ppm	θ	IE %	θ	IE %	θ	IE %	θ	IE %
50	0.608	60.8	0.581	58.1	0.49	49	0.402	40.2
100	0.643	64.3	0.613	61.3	0.506	50.6	0.447	44.7
150	0.676	67.6	0.657	65.7	0.552	55.2	0.499	49.9
200	0.721	72.1	0.681	68.1	0.618	61.8	0.553	55.3
250	0.764	76.4	0.724	72.4	0.657	65.7	0.607	60.7
300	0.794	79.4	0.763	76.3	0.681	68.1	0.658	65.8

3.3. Kinetic –thermodynamic dissolution parameter

The parameters of activation for dissolution process measured from Arrhenius plot as below:

$$k_{corr} = A \exp(E_a^*/RT) \quad (5)$$

E^*_a can be gotten from the slope of log (k_{corr}) against 1/T plots with and without various concentrations of the EHD as shown in Fig. 2. Data of E_a^* are reported in Table.2.

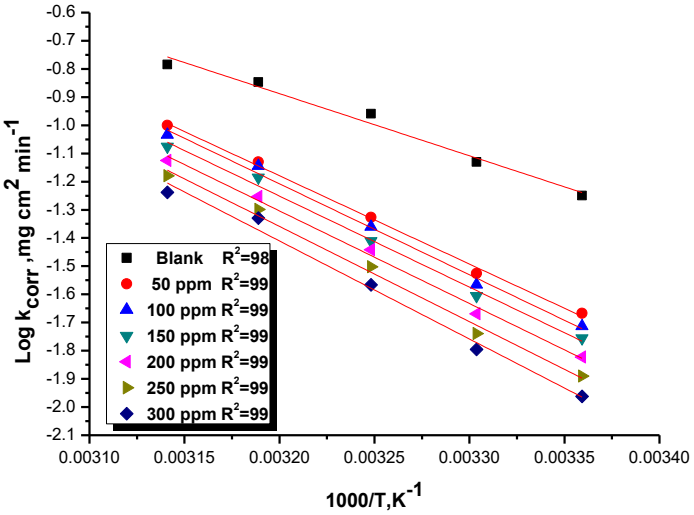

Figure 2. (Log k_{corr} vs. 1/ T) for dissolution of MS with and without various concentrations of EHD

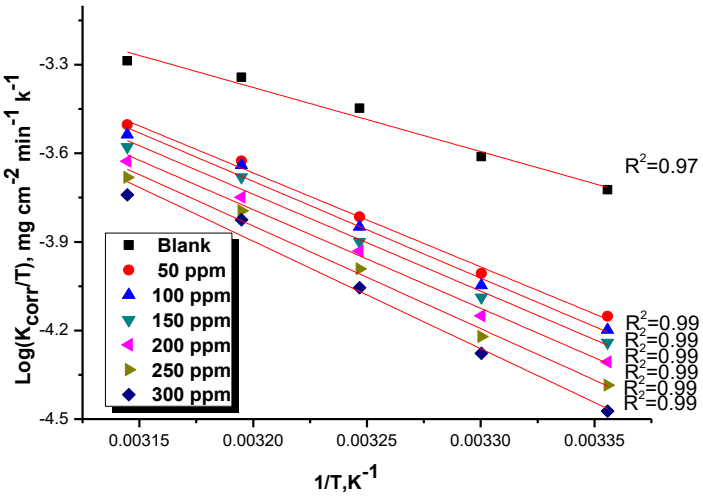

Figure 3. Transition-state for MS dissolution rates (k_{corr}) in 1 M HCl without and with different concentrations of EHD

Table 3. E^*_a, ΔH^* and ΔS^* value for MS dissolution with and without various concentrations of EHD in 1 M HCl

Conc., ppm	Activation parameters		
	E^*_a, kJ mol^{-1}	ΔH^*, kJ mol^{-1}	$-\Delta S^*$, J mol^{-1} K^{-1}
Blank	48.2	45.5	119
50	62	60.9	74.6
100	62.8	62.6	72.9
150	63.9	64.8	69.9
200	64.9	65.9	68.3
250	66.7	66.5	66.1
300	69.6	67.1	61.1

Examination of the data showed that E_a^* has higher values in existence of the EHD than that in its absence. This has attributed to the physical adsorption of EHD on MS surface. The transition state theory was used to compute the entropy and enthalpy of activation (Fig.3):

$$k_{corr} = (RT / Nh) \exp(\Delta S^*/R)\exp(-\Delta H^*/RT) \quad (6)$$

Where $\Delta S^*$and $\Delta H^*$are the activation entropy and enthalpy, respectively. The data verified in Table 2.

The higher E_a^* with growing concentrations and temperature of the drug (Table 2) is characteristic of physisorption. The + ve sign of ΔH^* indicates the endothermic process. ΔS^*data suggested that the activated complex at the rate determining step favor association rather than dissociation, indicating that a lower in the disordering [35].

3.4. Adsorption isotherms

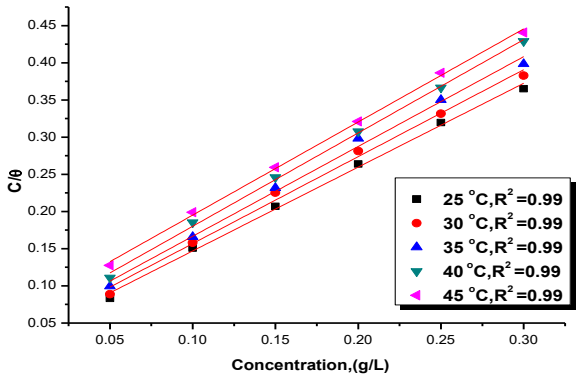

Figure 4. Langmuir adsorption plots for MS in 1M HCl including different concentrations of *EHD* at temperatures 298-318K

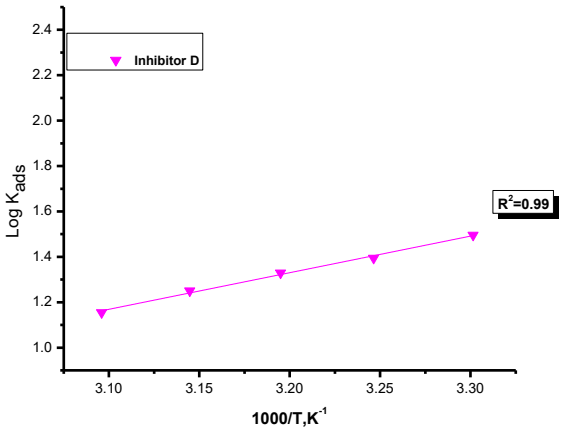

Figure 5. Plots of (*log* K_{ads}) against (1000/*T*) for the dissolution of MS in 1M HCl + *EHD concentrations*

Table 4. Adsorption parameters of *EHD* for MS surface generated from Langmuir adsorption isotherm at different temperatures

Temp. °C	K_{ads} M^{-1}	$-\Delta G^{\circ}_{ads}$ kJ mol^{-1}	$-\Delta H^{\circ}_{ads}$ kJ mol^{-1}	$-\Delta S^{\circ}_{ads}$ J mol^{-1} K^{-1}
25	147	18.7	36	63.3
30	133	18.4		60.9
35	112	18.1		59.9
40	85	17.8		58.2
45	65	17.4		56.5

Numerous isotherms had used to fit data, but the greatest fit was obtained to follow Langmuir adsorption isotherm which was shown in Fig.4 for the expired drug. Langmuir measured from the following relation:

$$C / \Theta = 1 / K_{ads} + C \quad (7)$$

Where the concentration of the EHD expressed as *C*, the adsorptive equilibrium constant expressed as K_{ads} and can be computed from the intercept of the variation between the C/Θ and C in Fig.4, the variation between C/Θ and C where Θ is the surface coverage, = *IE/100*. The relationship between K_{ads} against standard free energy expressed as ($\Delta G°_{ads}$), the $\Delta G°_{ads}$ can be estimated from Eq. 8, Fig. 4 explains the variation between log K_{ads} and 1/*T*.

The standard enthalpy $\Delta H°_{ads}$ and $\Delta S°_{ads}$ can be measured using Eq.8:

$$\Delta G^{\circ}_{ads} = \Delta H^{\circ} ads - T\Delta S^{\circ}_{ads} \quad (8)$$

By plotting ΔG°_{ads} vs T gave straight line (Fig. 5) with slope $\Delta S°_{ads}$ and intercept $\Delta H°_{ads}$. The +ve sign of $\Delta H°_{ads}$ ensures that the procedure of adsorption is an endothermic, and the – ve sign of $\Delta G°_{ads}$ (Table 4) means that adsorption happens spontaneously. The values of "a" were + ve at all temperatures showing that the attraction between the molecules of the drug adsorbed on MS surface [36].

3.5. EFM tests

EFM is a non-destructive corrosion test that can rapidly measure the data of corrosion current without prior knowledge of Tafel slopes [37]. The height of the peaks is a measure for (i_{corr}) and (i_{corr}) is a measure of protection quality %PE. In this technique, frequency is implemented and (i_{corr}) is measured. EFM is a non- liner response at which (i_{corr}) diminishes in going towards concentrations of *EHD*, owing to (i_{corr}) is the current resulted from dissolution so in case of *EHD* should have little values. The electrochemical parameters were detected and inscribed in Table 5, (CF-2 and CF-3) make internal check about the validity of the obtained results .Their values around 2 and 3 and it is an evidence for validity of results**.** Fig. 6 shows the EFM of MS in HCl solution including various concentrations of the EHD.

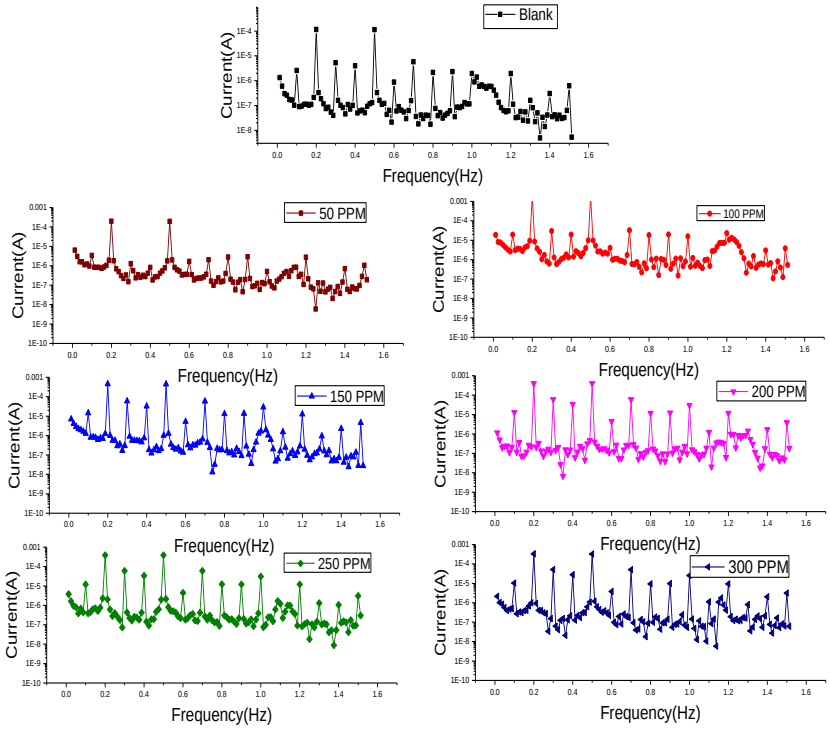

Figure 6. EFM spectra for MS in 1 M HCl with and without different concentrations of EHD at 25°C

Table 5. Electrochemical kinetic parameters obtained by EFM technique for MS with and without various concentrations of EHD in 1 M HCl at 25°C

Conc. ppm	i_{corr} μAcm^{-2}	β_a, $mVdec^{-1}$	β_c, $mVdec^{-1}$	C.R mpy	CF-2	CF-3	θ	%PE
Blank	777	105	126	355	1.8	2.90	---	---
50	245	85	95	132	2.0	3.0	0.685	68.5
100	212	77	98	126	1.9	2.9	0.727	72.7
150	199	73	90	115	2.0	3.0	0.744	74.4
200	144	71	98	101	1.8	2.9	0.815	81.5
250	133	76	91	98	1.9	2.9	0.829	82.9
300	120	89	96	55	2.1	3.1	0.846	84.6

3.6. EIS tests

Both Nyquist and Bode plots for MS corrosion in 1M HCl with and without varied concentrations of the drug were obtained and are shown in Fig. 7 (a, b). Impedance results occur by implementing AC potential and quantify the current passed within the cell. It is noticed from Nyquist plot that the curves appear semicircular. The frequency dispersion is responsible for the shape of the curve. The special shape of the Nyquist curves confirms that the MS corrosion is controlled by charge transfer process [38]. protection quality (%PE) can be computed by R_{ct} settled due to formation of protective layer on MS

surface among its advantages is ability of computing R_{ct}, C_{dl} that's by utilizing amplitude to decrease error of measurements Rct can be measured from Nyquist which is a relation between Z_{imag} and Z_{real} C_{dl} can be estimated from it by computing R_{ct} which is the diameter of the high frequency loop and owing to C_{dl} is inversely proportional to the R_{ct}. The results obtained prove that the expired drug works by forming the protective layer on the MS surface which modifies the MS/acid interface. Fig.8 is the equivalent circuit used to fit EIS data.

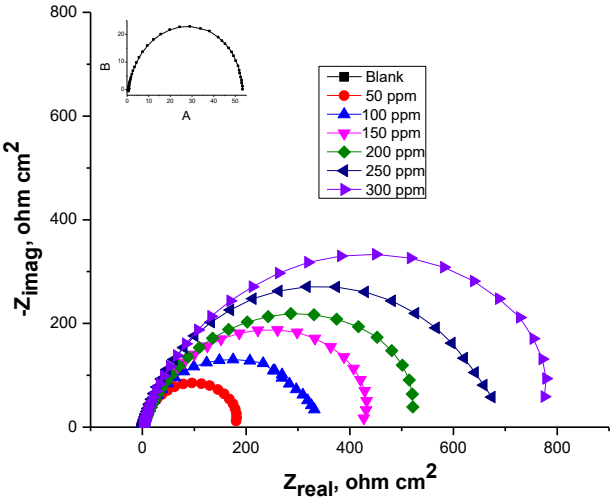

Figure 7a the Nyquist plots for the dissolution of MS in 1 M HCl at different concentrations of EHD at 25°C

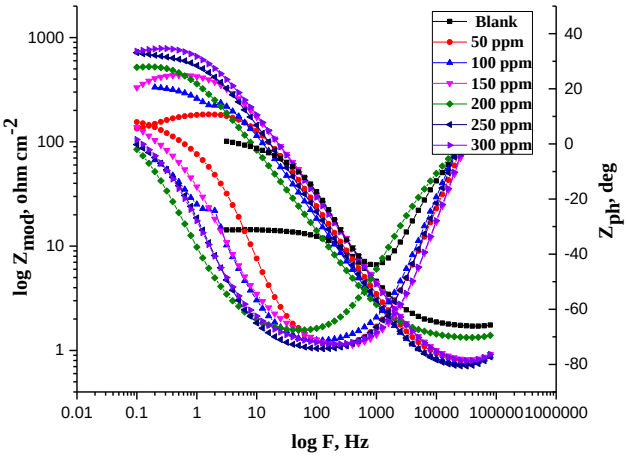

Figure 7b Bode plots for the corrosion of MS in 1 M HCl without and with various concentrations of EHD at 25°C

Table 6. EIS parameters obtained from EIS tests for MS in 1 M HCl with and without and without various concentrations of EHD

Conc., ppm	R_{ct}, Ω cm^2	C_{dl},x10^{-3}, µFcm^{-2}	θ	% PE
Blank	48.9	216	---	---

50	140	144	0.651	65.1
100	167	99	0.707	70.7
150	195	80	0.749	74.9
200	240	75	0.796	79.6
250	283	66	0.827	82.7
300	302	39	0.838	83.8

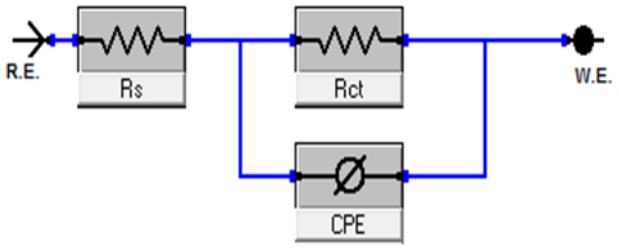

Figure 8. Equivalent model circuit utilized to fit experimental EIS data

3.7. PP tests

Tafel extrapolation curves for dissolution of MS was studied to examine the type of the inhibitor. The dissolution rate and dissolution current density (i_{corr}) of MS in the bare solution diminishes by adding EHD. Existence of the EHD raises both cathodic and anodic overvoltage and raises the shift in their values to the more negative and positive. The parallel cathodic and anodic Tafel curve in Fig. 9 confirms that there is no change in the mechanism. The small change in E_{corr} (less than 85 mV) with and without EHD and the small altered of the Tafel values, these indicate that EHD is considered as mixed-kind inhibitor, adsorbed on the cathodic locations of MS and diminishes the evolution of hydrogen gas. Further, the molecules of EHD adsorbed on anodic sites and diminish the anodic dissolution of MS.

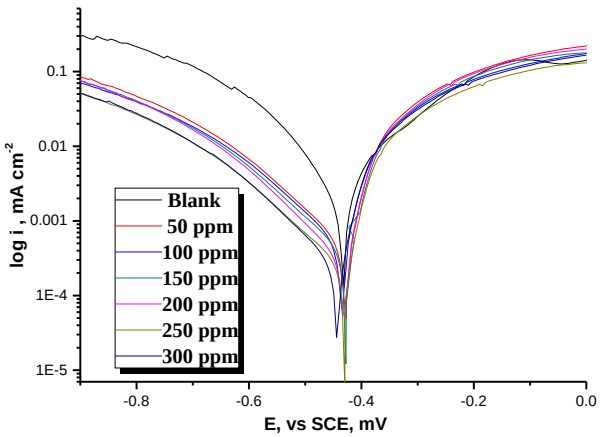

Figure 9. PP curves for the dissolution of MS in 1 M HCl with and without various concentrations of EHD at 25°C

Table 7. Data from PP of MS in 1 M HCl containing various concentrations of EHD at 25°C

Conc. ppm	i_{corr}, μA cm^{-2}	- E_{corr}, mV vs SCE	β_a mV dec^{-1}	β_c mV dec^{-1}	C.R mpy	Θ	% PE
Blank	995	433	120.0	151	390	--	--
50	276	421	116	147	272	0.723	72.3
100	240	420	120	149	265	0.759	75.9
150	230	423	118	151	257	0.769	76.9
200	195	415	115	152	245	0.804	80.4
250	167	418	120	155	224	0.832	83.2
300	141	415	117	153	167	0.858	85.8

3.8.1. AFM analysis

AFM is very important test to confirm the efficiency of the inhibitor on the MS surface. The 3D images for MS surface (standard coins a), MS immersed in 1M HCl (blank b) which found roughness (382 nm) and MS dipped in 1M HCl containing 300 ppm from EHD were possess roughness (186.9 nm) compared to the blank solution shown in Figure 10. The roughness data in gives clear sign that the MS surface appears smoother due to the adsorption of the EHD on the MS and forming the protective layer [40]. The roughness parameters for MS immersed in acid containing EHD inhibitor are somewhat greater than the standard coins but lower than blank sample and this approves the creation of protective film on the MS surface.

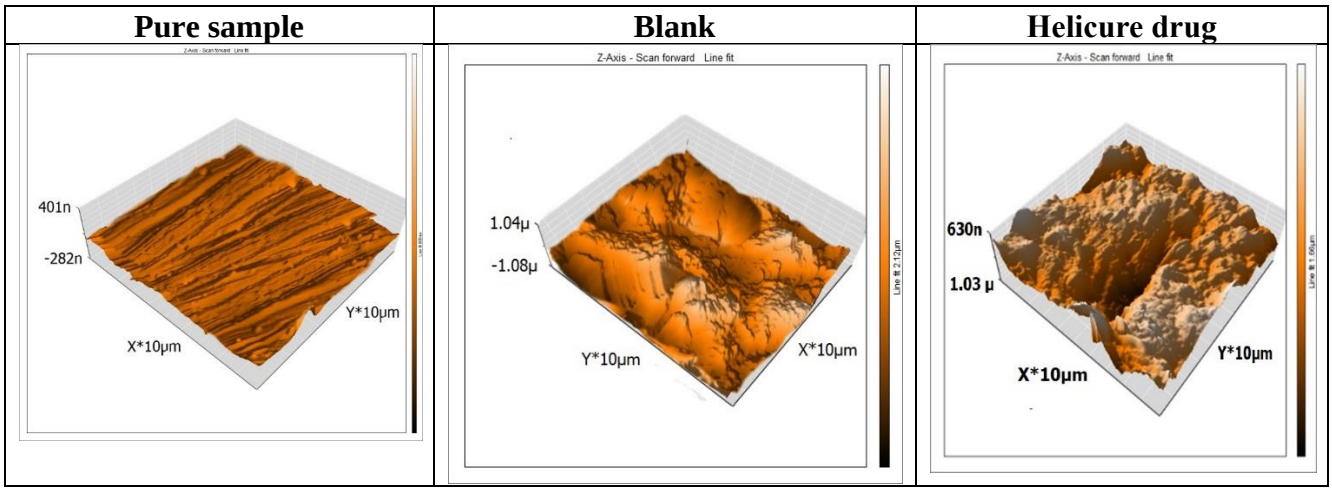

Figure 10 AFM images (3d) of (a) MS before dipping in acid (free) , (b) MS dipped in 2 M HCl alone (blank) and (c) MS dipped in 1M HCl at 300 ppm of EHD for 24 hours at 25°C

Table 8. AFM of investigated EHD at 300 ppm for 24 hours at 25ºC

Inhibitor		Sa	Sq	Sy	Sp	Sv	Sm
(a)	MS metal (free)	28	40	706	236	-291	-9.8
(b)	MS metal + 1 M HCl (blank)	382	501	3592	1361	-1703	-20.2
(C)	MS metal + 1 M HCl + 300 ppm EHD	186.9	244	1887	824	-106	-9.4

Where Sa is the roughness average, Sq is the root mean square, Sp is the peak height, Sm is the mean value, Sv is the valley depth and Sy is the peak-valley height

3.8.2 The FT-IR study

Figure 11 shows the FTIR spectra of the EHD inhibitor. The finger print spectra of the drug and the MS surface after engagement in 1M HCl + 300 ppm of EHD was gotten and compared to each other it was clearly clear that the same finger print of Helicure drug stock solution existing on MS surface except the lack of some functional group and it suggested to be due to reaction with HCl.

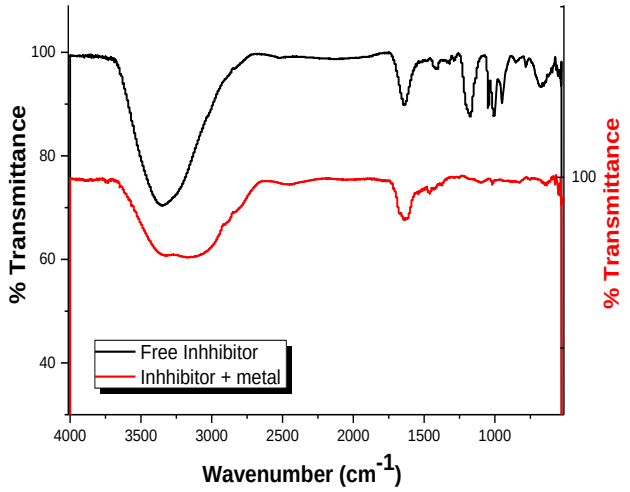

Figure 11. FT – IR spectrum of EHD before and after adsorption on the MS surface

3.9. Mechanism of corrosion protection

The adsorption of EHD drug molecules can be aspect to the attendance of polar unit having atoms of O and N and heterocyclic/aromatic rings. Therefore, the probable reaction centers are л-electrons of aromatic ring and unshared pair electron of hetero-atoms [41]. The possible description of the protection is due to adsorption process that has considered as the key of the mechanism of protection action. It might be plan that the drug molecules adhere to the MS surface. This leads to a lesser of the surface area available to corrode. Protection efficiency of the drug molecule relies on many the number of adsorption

active sites in the molecule and their charge density, molecular size, and mode of interaction with MS surface [42]. In acid solutions, the drug exists either as neutral molecules or in the form of protonated species. In general, two modes of adsorption could be considered. The relatively high IE of the drug can be attributing to the existence of phenyl ring as well as functional groups such as N, O and S atoms.

Table 9 gives a comparative study of the expired drugs used before as corrosion inhibitors for mild steel in HCl and H_2SO_4 solutions.

Table 9. A comparative chart listing the performance of some drugs as corrosion inhibitors

Drug	Metal/alloy	medium	PE%	Reference
Penciillin G	MS	H_2SO_4	73.7	[43]
Penciillin V	MS	H_2SO_4	63.3	[44]
Quinoline	MS	HCl	88.7	[45]
Cefalexin	MS	HCl	67.5	[46]
Ceftriaxone	MS	HCl	90.0	[47]
Cefotaxime	MS	HCl	90.0	[47]
Cefixime	MS	HCl	90.0	[48]
Helicure drug at 300 ppm	MS	HCl	85.8	Present work

4. CONCLUSIONS

Expired Helicure drug drug has found to be excellent inhibitor for the corrosion of MS in HCl acid media. The %IE increased with the rise in the dose of the drug and temperature. The values of E^*_a and ΔG^O showed that the drug is chemically adsorbed on the MS surface in HCl acid. PP data revealed that the drug was of mixed type. The EIS results supported the results obtained from WL, PP, EFM studies. R_{ct} values increased by adding the drug but C_{dl} decreased suggesting that the drug was adsorbed on the MS surface even at low concentrations.

References

1. A.Y.Musa, A.A. Khadom, A.H. Kadhum, *J. Taiwan Inst. Chem. Eng*., 41(2010) 126.
2. M.A.Ameer, A.M.Fekry, *Int. J. Hydrogen Energy*, 35 (2010) 11387.
3. R.T.Loto, C.A.Loto, A.P.I.Popoola, *Journal of Materials and Environmental Science*, 3 (2012)885.
4. D.G.Ladha, U.J. Naik, N.K.Shah, *Journal of Materials and Environmental Science*, 4 (2013) 701-708. .
5. N.Hajjaji, I.Ricco, A.Srhiri, A.Lattes, M.Soufiaoui, A.Benbachir, *Corrosion*, 49 (1993) 326.
6. M.Elachouri, M.S.Hajji, M.Salem, S. Kertit, R.Coudert, E.M.Essassi, *Corros Sci*, 37 (1995)381.
7. H.Luo, Y.C.Guan, K.N.Han, *Corrosion*, 54 (1998) 619.
8. M.A.Migahed, E.M.S.Azzam, A.M.Al-Sabagh, *Mater. Chem. Phys.*, 85 (2004) 273.
9. M.M.Osman, A.M. Omar. A.M.Al-Sabagh, *Mater. Chem. Phys*., 50 (1997) 271.
10. F. Zucchi, G.Trabanelli, G.Brunoro, *Corros Sci.*, 33 (1992) 1135.
11. R.F.V.Villamil, P.Corio, J.C.Rubim, M.L.Siliva Agostinho, *J Electroanal Chem*, 472 (1999)112.
12. T.P.Zhao, G.N.Mu, *Corros Sci.*, 41 (1999)1937.

13. S.S.Abd El Rehim, H.Hassan, M.A.Amin, *Mater. Chem. Phys*., 70(2001) 64.
14. S.S.Abd El Rehim, H. Hassan, M.A.Amin, *Mater Chem Phys*., 78 (2003) 337.
15. R. Guo, T.Liu, X.Wei, *Colloids Surf*. 209 (2002) 37.
16. V.Branzoi, F.Golgovici, F.Branzoi, *Mater. Chem. Phys*., 78 (2002) 122.
17. T.F.Bentiss, M.Lagrenee, *Corros Sci*., 42 (2000)127.
18. Christopher M.A.B., Isabel Jenny A.R., *Corros Sci*., 36: (1994) 9153.
19. M.Elachouri, M.Hajji, M.Salem, S. Kertit, J.Aride, R.Coudert, E.Essassi, *Corrosion*, 52 (1996)103.
20. A.S.Algaber, E.M.El-Nemma, M.M.Saleh, *Mater. Chem. Phys*., 86 (2004) 26.
21. R.Oukhrib, B.El Ibrahimi, H.Bourzi, K.El Mouaden, A.Jmiai, S.El Issami, L.Bammou, L.Bazzi, *JMES*, 8 (1) (2017) 195.
22. A. M. Al-Azzawi, K.K. Hammud, *IJRPC*, 6(3) (2016) 3912.
23. L.El Ouasif, I.Merimi, H.Zarrok, M.El ghoul, R.Achour, M.Guenbour, H.Oudda, F.El-Hajjaji, B.Hammouti, *J Mater Environ Sci*., 7 (8) (2016) 2718.
24. U.M.Sani, U.U.Sman, *International J. Novel Res.Phys.Chem.Math*. 3(3) (2016) 30.
25. A.M.Kolo, U.M. Sani, U.Kutama, U.Usman, *the Pharm. Chem. J*., 3(1) (2016)109-119.
26. P.O.Ameh, U.M.Sani, *Journal of Heterocyclics*, 1(1) (2015) 2.
27. R.Kushwah, R.K.Pathak, *Inter.J. Emerg. Technol.Adv. Eng*., 4(7) (2014) 880.
28. A.S.Fouda, M.N.EL-Haddad, Y.M.Abdallah, *IJIRSET*, 2(12) (2013)7073.
29. Ofoegbu S.U., Ofoegbu P.U., *ARPN J.Eng.Appl. Sci*., 7 (3) (2012)272.
30. G.N.Mu, T.P.Zhao, M.Liu, T. Gu, *Corrosion*, 52 (1996)853.
31. Lipkowski J., Ross P.N., Adsorption of Molecules at Metal Electrodes, VCH, New York, (1992)
32. SLFA Da Costa, S.M.L. Agostinho, *Corrosion*, 45 (1989)472.
33. J.Aljourani, K.Raeissi, M.A. Golozar, *Corros. Sci*., 51 (2009)1836.
34. M.Lebrini, F.Bentiss, H.Vezin, M.Lagrenee, *Corros. Sci.,* 48 (2006)1279.
35. L.Tang, X.Li, Y.Si, G.Mu, G. Liu, *Mater. Chem. Phys*., 95 (2006) 29
36. G.A.Caigman, S.K.Metcalf, E.M.Holt,,,*J Chem. Cryst*., 30 (2000)415.
37. G.Trabanelli, C.Montecelli, V.Grassi, A.Frignani, *J. Cem. Concr. Res*., 35 (2005)1804.
38. F.M.Reis, H.G.De Melo, I.Costa, *Electrochim Acta*, 51 (2006)1780.
39. M.Lagrenee, B.Mernari, M.Bouanis, M.Traisnel, F.Bentiss, *Corros. Sci.,* 44 (2002)573.
40. H.Ma, S.Chen, L.Zhao, S.Li, D.Li, *J. Appl. Electrochem*., 32 (2002)65.
41. A.S.Fouda, H. Ibrahim, M.Atef, *Results in Physics*, 7 (2017)3408.
42. H.Patmore, A.Jebreel, S.Uppal, C.H.Raine, P.Whinney, *Am.J.Otolaryngol*, 31(5) (2010)376
43. G.J.Ridder, C.Breunig, J.Kaminsky, J.Pfeiffer, *European archives of oto-rhino-laryngology*, 272(5) (2015)1269.
44. D.H.Kraus, S.J.Rehm, S.E.Kinney, *the Laryngoscope*, 98(9) (1988) 934.
45. P.Sharma, K.K.Agarwal, S.Kumar, H.Singh, C.Bal, *SPECT and CT. Jpn. J. Radiol*., 31(2) (2013) 81.
46. M.P. Stokkel, C.N.Boot, B.L.Van Eck-Smit, *Laryngoscope* 106(3 Pt 1) (1996) 338.
47. M.P.Clark, P.M.Pretorius, I. Byren, C.A. Milford, *Skull Base* 19(4) (2009) 247.
48. N.C.Okpala, Q.H.Siraj, E.Nilssen, M.Pringle, *J. Laryngol Otol*, 119(1) (2005)71.